respectively. This corresponds to 62 μGy/mAs and 9.7 μGy/mAs.
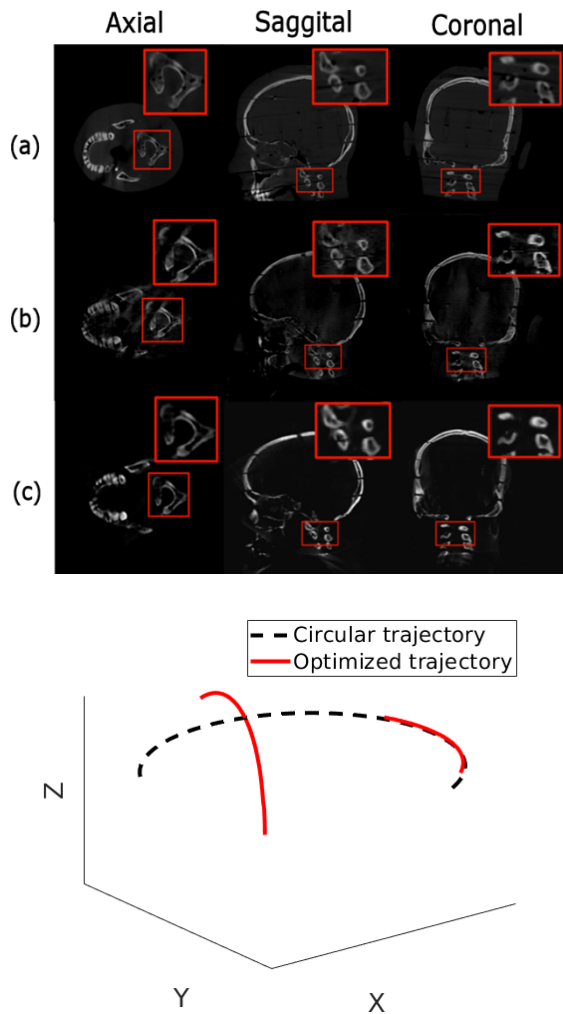
Conclusion

Our dosimetry results showed the CTDI per mAs delivered by the optimized trajectory was six times lower than by the standard trajectory. We demonstrated that applying a minimal dedicated set of projections with optimized orientations in 3D space is sufficient to localize targets and has the potential for low dose CBCT-guided therapies.

PO-1702 Optimizing the generation of brain pseudo-CT from MRI based on a highly efficient 3D neural network

E. Alvarez Andres[1,2,3], L. Fidon[1], M. Vakalopoulou[4], M. Lerousseau[2,3,4], A. Carré[2,3], R. Sun[2,3,4,5], A. Beaudre[2], E. Deutsch[3,5], N. Paragios[1], C. Robert[2,3]
[1]TheraPanacea, Radiotherapy, Paris, France ; [2]Department of Medical Physics, Gustave Roussy - Paris-Saclay University, Villejuif, France ; [3]U1030 Molecular Radiotherapy, Paris-Sud University - Gustave Roussy - Inserm - Paris-Saclay University, Villejuif, France ; [4]MICS Laboratory, CentraleSupélec- Paris-Saclay University, Gif-sur-Yvette, France ; [5]Department of Radiotherapy, Gustave Roussy - Paris-Saclay University, Villejuif, France

Purpose or Objective

Brain pseudo Computed Tomography (pCT) were generated from Magnetic Resonance Imaging (MRI) using a 3D convolutional neural network. The contributions of this study are threefold: assessing the best suited MRI input sequence, benchmarking different MRI standardization methods and inferring the minimal number of patients of the training set for a high quality pCT.

Material and Methods

402 institutional brain tumor patients were retrieved yielding to associations of 182 CT/T1 weighted MRI (T1), 181 CT/contrast enhanced T1 weighted MRI (T1-Gd) and 39 CT/T1/T1Gd. These data were used to train, validate and test a modified version of the 3D neural network HighResNet (Li et al., 2017). First, to assess the most informative MR input sequence, two models were developed either based on T1 MRI sequence only (218 patients) or T1-Gd only (217 patients) cohorts. Then, three standardization strategies, namely Histogram Based (HB), Zero Mean Unit Variance (ZMUV) and No Standardization (NS), were compared based on training, validation and testing sets composed of 242, 81 and 79 patients respectively. Finally, further models were trained on subsets of the training set (242, 121, 60, 30, 15 patients) and compared based on fixed validation and testing sets (81 and 79 patients respectively) to assess the behavior of the subsequent models performance in function of the input size. Comparisons between the ground-truth CT and pCT were conducted computing the Mean Absolute Error (MAE) within four areas (whole head, air, water and bone), global 1%/1mm, 2%/2mm, 3%/3mm gamma indexes and Dose Volume Histograms (DVH) differences based on planning target volume. Paired samples Wilcoxon tests were performed as statistical analysis.

Results

Figure 1 presents qualitative results.
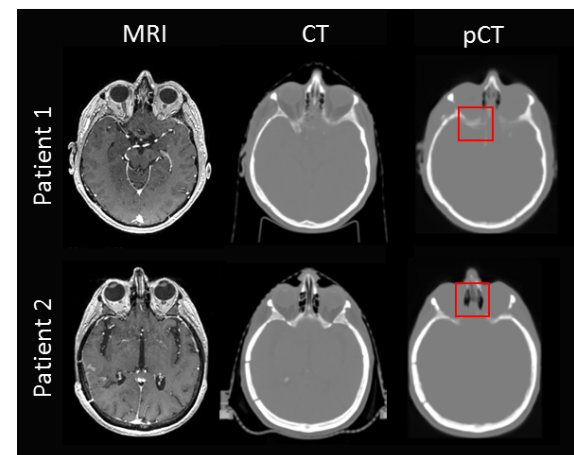
Fig. 1. MRI, ground-truth CT and pCT. The red squares highlight incorrect reconstructed areas.

Reported results are presented such as [median, interquartile range]. Head MAE of [80Hounsfield Units (HU), 27HU] and [84HU, 28HU] were achieved for the T1 only and T1-Gd only based experiments respectively. Gamma indexes differences were not found significant. Regarding the three standardization strategies, head MAE equal to [89HU, 27HU], [81HU, 26HU], [92HU, 27HU] were obtained for the HB, ZMUV and NS respectively, proving the significant superiority of the ZMUV approach (p-values≤0.0001). All DVH differences medians were below 0.25%. Finally, Figure 2 presents the MAE distribution computed from the training set size experiment, and suggests the use of at least 121 patients in the training set for this study.
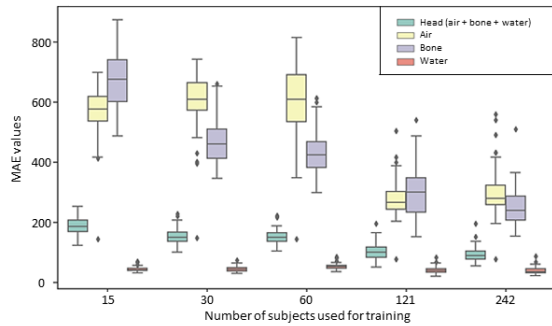
Fig. 2. MAE distribution evolution when varying the number of patients in the training set.

Conclusion

Competitive pCT were generated when combining ZMUV standardization with a training set containing at least about 120 patients. Using T1 only or T1-Gd only MR sequences did not impact the quality of dosimetric maps calculated from pCT.

PO-1703 Renal positional probability mapping using ultra-fast volumetric 4D-MRI for MRgRT

J. Yuan[1], O.L. Wong[1], R.Y.W. Ho[1], Y. Zhou[1], K.Y. Cheung[1], S.K. Yu[1]
[1]Hong Kong Sanatorium & Hospital, Medical Physics and Research Department, Happy Valley, Hong Kong SAR China

Purpose or Objective

Current orthogonal-cine MRI on product MRI-guided-radiotherapy (MRgRT) platforms is incapable of obtaining volumetric motion information of organ. This study aims to investigate the positional probability map (PPM) of kidney under respiratory motion using an ultra-fast volumetric 4D-MRI for MRgRT applications.

Material and Methods

9 healthy volunteers underwent free-breathing abdominal scans on a 1.5T MR-sim with RT positioning using a volumetric CAIPIRINHA-VIBE 4D-MRI (TE/TR=0.5/1.8ms, flip angle=5°, 56 axial-slices/volume, voxel size=2.7x2.7x4mm^3, temporal resolution= ~0.6s, 144 time frames). Left and right kidneys were masked on the 1st end-exhalation frame as references and images at each frame were linearly registered to the references to create the dynamic renal binary masks. Dynamic renal PPM was calculated by the number of frames that a voxel had been occupied by kidney divided by the total elapsed frames, i.e. $PPM_j = (M_1 + ... + M_j) \times 100\%/j$. (binary mask value $M_j=1$ or 0, j: frame index). Probabilistic renal volume with $PPM \geq i\%$ (Vi%) was calculated using the first 44 frames as baseline, then dynamically updated at every frame j>44. Subject-specific renal Vi% (i=0, 5, 25, 50, 75, 100) was calculated and compared to the reference kidney volumes (Vk). Dynamic Vi% and their variability with time (mean±sd) were assessed. Signed rank test was performed to compared Vi% (i=0, 5, 25, 50, 75, 100) between the left and right kidney.

Results

Group averaged probabilistic renal volume V0%, V5%, V25%, V50%, V75% and V100% relative to Vk using all time frames for two kidneys were (L: 1.33±0.11; R: 1.32±0.06), (L: 1.23±0.07; R: 1.21±0.05), (L: 1.12±0.03; R: 1.11±0.03), (L: 1.00±0.01; R: 1.00±0.01), (L: 0.88±0.03; R: 0.89±0.02) and (L: 0.70±0.08; R: 0.71±0.05), respectively. V5% implied that an extra ~20% of the kidney volume should be expanded from the reference position to cover the 95% probabilistic renal motion range. The volume that kidney always occupied during respiration is only ~0.7Vk, as indicated by V100%. No significant differences were observed in all Vi% between left and right kidneys. All time-resolved dynamic probabilistic renal volumes were quite stable within the scan time, almost all ≤2%Vk, after the baseline established on the first 44 time frames. This indicated that a short scan duration of ~27s might be sufficient to accurately estimate the renal respiratory PPM, while further study is warranted to investigate the influence of irregular respiratory motion on the time-resolved PPM based on real cancer patients.

i	Vk(L,R) [mm³]	Vi/Vk (L,R)	Vmax/Vk (L,R)	Vmin/Vk (L,R)	Mean Stability Vi/Vk (L,R)	CV Vi/Vk (L,R)
100	(160 ± 34, 154 ± 27)	(0.70 ± 0.08, 0.71 ± 0.05)	(0.70 ± 0.09, 0.71 ± 0.05)	(0.74 ± 0.06, 0.75 ± 0.06)	(0.72 ± 0.06, 0.73 ± 0.05)	(1.70 ± 1.39 %, 1.78 ± 1.36 %)
75	(160 ± 34, 154 ± 27)	(0.88 ± 0.03, 0.89 ± 0.02)	(0.86 ± 0.02, 0.88 ± 0.01)	(0.90 ± 0.03, 0.90 ± 0.02)	(0.88 ± 0.03, 0.89 ± 0.02)	(0.93 ± 0.69 %, 0.65 ± 0.56 %)
50	(160 ± 34, 154 ± 27)	(1.00 ± 0.01, 1.00 ± 0.01)	(0.99 ± 0.01, 1.00 ± 0.01)	(1.01 ± 0.01, 1.01 ± 0.02)	(1.00 ± 0.01, 1.00 ± 0.01)	(0.33 ± 0.25 %, 0.36 ± 0.49 %)
25	(160 ± 34, 154 ± 27)	(1.12 ± 0.03, 1.11 ± 0.03)	(1.10 ± 0.02, 1.10 ± 0.03)	(1.13 ± 0.03, 1.11 ± 0.03)	(1.12 ± 0.02, 1.11 ± 0.03)	(0.48 ± 0.38 %, 0.48 ± 0.39 %)
5	(160 ± 34, 154 ± 27)	(1.24 ± 0.07, 1.21 ± 0.05)	(1.22 ± 0.07, 1.20 ± 0.05)	(1.25 ± 0.07, 1.23 ± 0.06)	(1.24 ± 0.07, 1.21 ± 0.06)	(0.56 ± 0.39 %, 0.56 ± 0.39 %)
0	(160 ± 34, 154 ± 27)	(1.34 ± 0.11, 1.32 ± 0.06)	(1.29 ± 0.11, 1.28 ± 0.07)	(1.34 ± 0.11, 1.32 ± 0.06)	(1.32 ± 0.11, 1.30 ± 0.06)	(1.16 ± 0.83 %, 1.07 ± 0.92 %)